Maria João Matos, Santiago Vilar, Saleta Vazquez-Rodriguez, Sonja Kachler, Karl-Norbert Klotz, Michela Buccioni, **Giovanna Delogu**, Lourdes Santana, Eugenio Uriarte, Fernanda Borges

Structure-based optimization of coumarin hA3 adenosine receptor antagonists

Journal of Medicinal Chemistry, **2020**, 63(5), 2577-2587. **ISSN**: 00222623; **DOI**: **Scopus code**: 2-s2.0-85076242889

The publisher's version is available at: 10.1021/acs.jmedchem.9b01572;
http://dx.doi.org/[inserire DOI]

Structure-based optimization of coumarin hA3 adenosine receptor antagonists

Maria João Matos,[a,b,*] Santiago Vilar,[b] Saleta Vazquez-Rodriguez,[b] Sonja Kachler,[c] Karl-Norbert Klotz,[c] Michela Buccioni,[d] Giovanna Delogu,[e] Lourdes Santana,[b] Eugenio Uriarte,[b,f] Fernanda Borges[a,*]

[a] CIQUP/Department of Chemistry and Biochemistry, Faculty of Sciences, University of Porto, 4169-007 Porto, Portugal

[b] Department of Organic Chemistry, Faculty of Pharmacy, University of Santiago de Compostela, 15782 Santiago de Compostela, Spain

[c] Institute of Pharmacology and Toxicology, University of Würzburg, 97078 Würzburg, Germany

[d] School of Pharmacy, Medicinal Chemistry Unit, University of Camerino, 62032 Camerino, Italy

[e] Department of Life Sciences and Environment - Section of Pharmaceutical Sciences, University of Cagliari, 09124 Cagliari, Italy

[f] Instituto de Ciencias Químicas Aplicadas, Universidad Autónoma de Chile, 7500912 Santiago, Chile

Abstract. Adenosine receptors are involved in several physiological processes. Molecules able to selectively modulate one of these receptors represent promising multifunctional agents to treat or slow down the progression of different diseases. Some of these compounds, including A1 and A3 agonists, may have clinical use in the treatment of disorders of the nervous system, such as chronic pain, neurodegeneration and brain injury. 3-Arylcoumarins have already been studied as neuroprotective agents by our

group. Here, differently 8-substituted 3-arylcoumarins are complementarily studied as ligands of adenosine receptors, performing radioligand binding assays. Among the synthesized compounds, selective A_3 receptor antagonists have been identified. 3-(4-Bromophenyl)-8-hydroxycoumarin (compound **4**) proved to be the most potent and selective A_3 receptor antagonist (K_i = 258 nM). An analysis of its X-ray diffraction provided detailed information on the structure, phase, preferred crystal orientations, and other structural parameters. Interestingly, the presence of a hydroxyl group at position 8 of the coumarin scaffold highly increases the activity on A_3 receptors. Further evaluation of a selected series of compounds indicated that it is the nature and position of the substituents that determine their activity and selectivity. Theoretical modeling calculations corroborate and explain the experimental data, suggesting this novel scaffold has desirable properties for the development of potential multitarget drug candidates.

Keywords: 3-Arylcoumarins • Perkin reaction • Perkin-Oglialoro reaction • Adenosine antagonists • Molecular modeling

INTRODUCTION

Adenosine is a purinergic nucleoside acting as a ubiquitous regulator of different tissues and cell activities.[1] This purine controls important pathophysiological functions via four distinct adenosine receptor subtypes (A_1, A_{2A}, A_{2B} and A_3).[2] Adenosine is the endogenous, nonselective adenosine receptor agonist that is short-lived in the body, while its metabolite inosine, following the action of adenosine deaminase, weakly activates the A_3 receptor.[3]

Adenosine receptors, a class of G protein-coupled receptors (GPCR), have long been considered as promising therapeutic targets in a wide range of conditions,[4] from cerebral diseases to cancer, including inflammatory and immunological disorders.[5,6] There is a huge variety of chemical entities designed as adenosine receptor ligands, both directly

group. Here, differently 8-substituted 3-arylcoumarins are complementarily studied as ligands of adenosine receptors, performing radioligand binding assays. Among the synthesized compounds, selective A_3 receptor antagonists have been identified. 3-(4-Bromophenyl)-8-hydroxycoumarin (compound **4**) proved to be the most potent and selective A_3 receptor antagonist (K_i = 258 nM). An analysis of its X-ray diffraction provided detailed information on the structure, phase, preferred crystal orientations, and other structural parameters. Interestingly, the presence of a hydroxyl group at position 8 of the coumarin scaffold highly increases the activity on A_3 receptors. Further evaluation of a selected series of compounds indicated that it is the nature and position of the substituents that determine their activity and selectivity. Theoretical modeling calculations corroborate and explain the experimental data, suggesting this novel scaffold has desirable properties for the development of potential multitarget drug candidates.

Keywords: 3-Arylcoumarins • Perkin reaction • Perkin-Oglialoro reaction • Adenosine antagonists • Molecular modeling

INTRODUCTION

Adenosine is a purinergic nucleoside acting as a ubiquitous regulator of different tissues and cell activities.[1] This purine controls important pathophysiological functions via four distinct adenosine receptor subtypes (A_1, A_{2A}, A_{2B} and A_3).[2] Adenosine is the endogenous, nonselective adenosine receptor agonist that is short-lived in the body, while its metabolite inosine, following the action of adenosine deaminase, weakly activates the A_3 receptor.[3]

Adenosine receptors, a class of G protein-coupled receptors (GPCR), have long been considered as promising therapeutic targets in a wide range of conditions,[4] from cerebral diseases to cancer, including inflammatory and immunological disorders.[5,6] There is a huge variety of chemical entities designed as adenosine receptor ligands, both directly

acting as agonists, antagonists, and indirect modulators.[7] Regadenoson (CVT-3146), a selective agonist of the A_{2A} receptor is used to induce stress in cardiac imaging, and istradefylline (KW-6002), a xanthine antagonist of the A_{2A} receptor, has been approved in Japan for treating Parkinson's disease.[8,9] The increasing knowledge on the molecular biology of A_3 receptors has provided important pieces of evidence to consider this receptor as a novel therapeutic target.[10] This enables rational design and development of potent and selective A_3 receptor antagonists as promising therapeutic solutions for a variety of diseases.[11] An increasing number of reports suggest an important role for A_3 receptor in mediating adenosine action in the central nervous system.[12,13] A_3 receptors are also known to induce a robust anti-inflammatory effect in experimental animal models.[14] These particular activities aroused our attention, since our research group has been working in the area of age-related pathologies, in particular vascular, inflammatory and neurodegenerative diseases.[15]

Based on the background of our research group regarding differently substituted coumarins as potential adenosine receptor ligands,[16,17,18,19,20,21] and in the potential of some of these compounds as inhibitors of several enzymes (monoamine oxidase B, acetylcholinesterase and butyrylcholinesterase) involved in neurodegenerative diseases and as neuroprotectors, in the current work we describe a selected series of coumarin derivatives bearing a wide variety of substituents as modulators of adenosine receptors. In particular, the revealing achievements of our last work on the interesting activity of 8-substituted 3-arylcoumarins (Figure 1) have been the inspiration for the progression of this study.[21] Design, synthesis, pharmacological evaluation, docking calculations, and structure-activity relationship studies of a selected series of 8-substituted 3-arylcoumarins, were carried out.

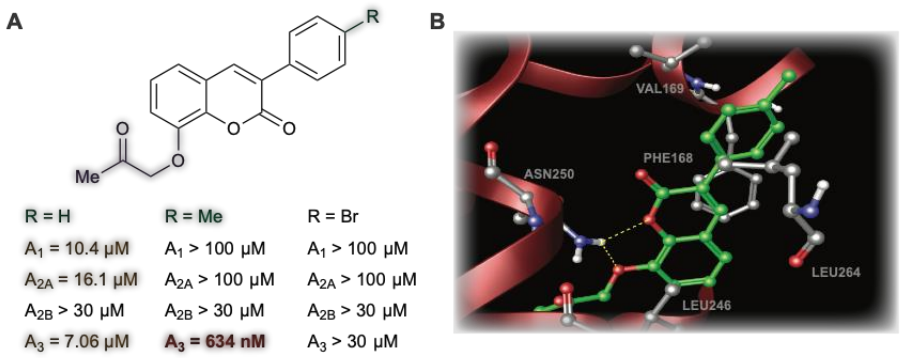

Figure 1. Previous results from the group on the potential of 8-substituted 3-arylcoumarins as adenosine ligands at adenosine 7TM receptors. **A.** Three 8-(2-oxopropoxy)-3-arylcoumarins with different affinity profiles. **B.** Hypothetical binding mode for 8-(2-oxopropoxy)-3-(*p*-tolyl)coumarin in the hA3 protein pocket. Color code: pale orange – activity in the micromolar range; red – activity in the nanomolar range.

RESULTS AND DISCUSSION

Chemistry. Compounds **1-27** were efficiently synthesized according to the synthetic strategies outlined in Figure 2A. In general, these compounds were obtained by a classic Perkin (compounds **1-3**, **5-14**, **16** and **17**) and Perkin-Oglialoro (compounds **18-22**) synthetic reactions. Further hydrolysis of the ethoxy derivatives (compounds **4** and **15**) and acetoxy derivatives (compounds **23-27**) allowed the obtention of the hydroxyl derivatives.[22,23,24,25]

Perkin condensation of different *ortho*-hydroxybenzaldehydes with the adequate arylacetic acids, using *N,N'*-dicyclohexylcarbodiimide (DCC) as dehydrating agent, afforded the 3-arylcoumarins **1-3**, **5-14**, **16** and **17**. Afterwards, compounds **4** and **15** were obtained by acidic hydrolysis from the respective ethoxy derivatives **3** and **14**, using hydriodic acid (HI) 57% in the presence of acetic acid (AcOH) and acetic anhydride (Ac_2O).

Perkin-Oglialoro condensation of different commercially available *ortho*-hydroxybenzaldehydes and arylacetic acids, using potassium acetate (CH_3CO_2K) in acetic anhydride (Ac_2O), under reflux, for 16 h, afforded the acetoxy-3-arylcoumarins **18-22**. Acetylation of the hydroxyl groups and pyrone ring closure occur simultaneously under these conditions. The hydrolysis of the obtained acetoxy derivatives, in the presence of aqueous hydrochloric acid (HCl) and methanol (MeOH), under reflux, for 3 h, allowed obtaining the hydroxyl substituted 3-arylcoumarins **23-27**.

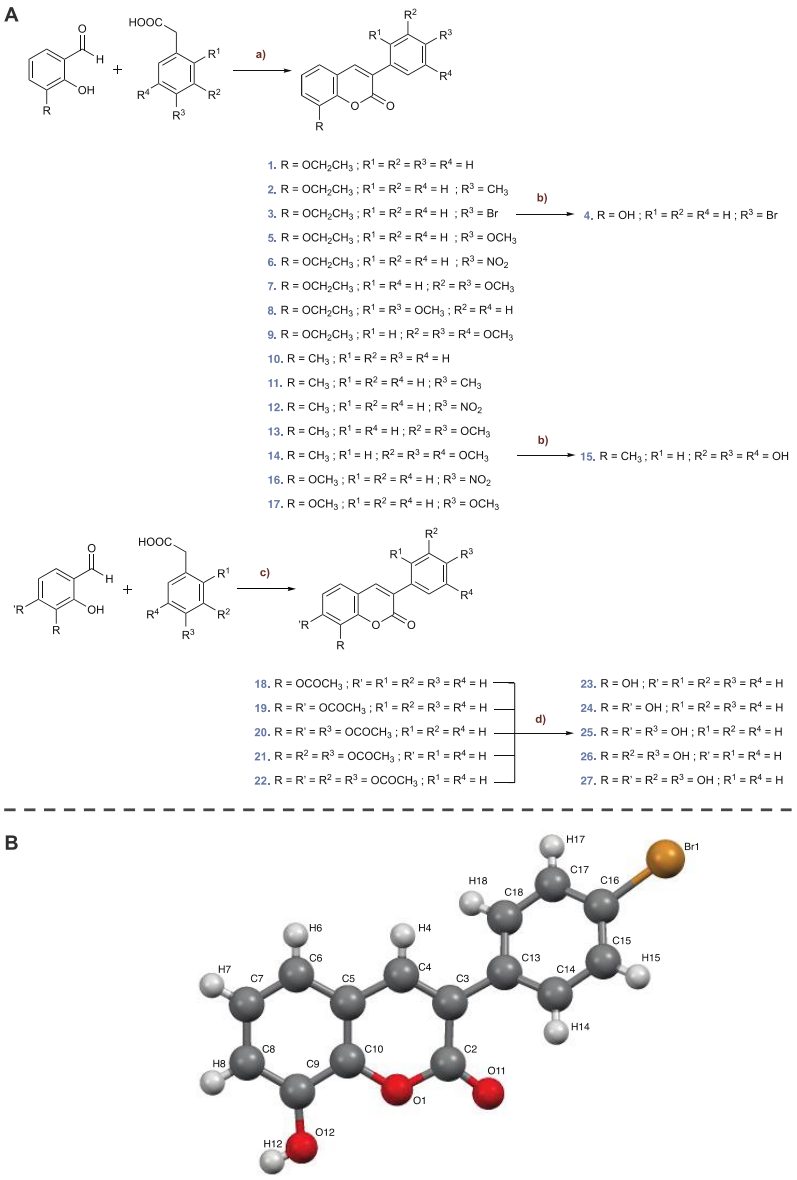

Figure 2. A. Scheme of the synthetic methodologies. Reagents and conditions: a) DCC, DMSO, 110 ºC, 24 h. b) HI, AcOH, Ac_2O, reflux, 3 h. c) CH_3CO_2K, Ac_2O, reflux, 16 h; d) HCl, MeOH, reflux, 3 h. **B.** Molecular structure of compound **4**, showing the atom-numbering scheme used in the X-ray study.

The structural analyses of compound **4** by X-ray crystallography (CCDC number 1937910)[26] corroborated the NMR information. This molecule is a coumarin derivative with a *p*-bromophenyl substituent at position 3 of the coumarin ring and a hydroxyl group at position 8, as seen in the chemical scheme (Figure 2B). The dihedral angle between both planes of the 3-arylcoumarin scaffold (~36.6±2.1°) may reveal some important information on the possible binding pose of compound **4** to the receptor, being typical of these family of molecules.[27] In addition, the C3—C13 bond length is typical from the 3-arylcoumarins 1.483 Å. This value is the same as the previously reported for the 3-phenylcoumarin, crystalized by our research group.[27] Also, the planarity of the coumarin moiety is evident by the torsion angles values between their carbons. Besides the interest in organic chemistry and structural elucidation, the deep structural knowledge of a molecule can be a significant tool for the understanding of its potential affinity and/or selectivity for particular receptors. All the details of the synthetic methodologies and characterization of the compounds are described in the experimental section.

Pharmacological study. The affinity of the newly described coumarins for A_1, A_{2A}, and A_3 adenosine receptors was tested in radioligand binding assays. The affinity for the A_{2B} receptor was determined in a functional assay (inhibition of agonist-stimulated adenylyl cyclase activity).[28,29] The detailed methodology is described in the experimental section. The binding data for A_1, A_{2A} and A_3 adenosine receptors are shown in Table 1. None of the derivatives showed measurable affinity for the A_{2B} receptor (IC_{50} > 30 μM, data not shown).

Table 1. Binding affinity (K_i values) of the studied coumarins **1-27** and reference compounds for human A_1, A_{2A} and A_3 adenosine receptors expressed in Chinese hamster ovary (CHO) cells.

Compound	R	R'	R_1	R_2	R_3	R_4	hA_1 (μM)	hA_{2A} (μM)	hA_3 (μM)
1	OCH_2CH_3	-	H	H	H	H	22.1 (18.0-27.1)	55.0 (36.4-83.1)	22.5 (14.0-36.3)
2	OCH_2CH_3	-	H	H	CH_3	H	> 100	> 60	3.93 (2.57-6.01)
3	OCH_2CH_3	-	H	H	Br	H	> 100	> 100	> 100
4	OH	-	H	H	Br	H	> 100	> 100	**0.258 (0.143-0.468)**
5	OCH_2CH_3	-	H	H	OCH_3	H	> 100	> 100	5.32 (3.68-7.68)
6	OCH_2CH_3	-	H	H	NO_2	H	> 100	> 100	> 100
7	OCH_2CH_3	-	H	OCH_3	OCH_3	H	> 100	> 100	13.7 (9.55-19.6)
8	OCH_2CH_3	-	OCH_3	H	OCH_3	H	> 100	> 100	16.6 (10.5-26.1)
9	OCH_2CH_3	-	H	OCH_3	OCH_3	OCH_3	> 100	> 100	9.05 (6.05-13.5)
10	CH_3	-	H	H	H	H	14.8 (9.34-23.3)	42.1 (33.6-52.7)	17.0 (11.2-25.7)
11	CH_3	-	H	H	CH_3	H	> 100	> 100	16.6 (10.2-26.9)
12	CH_3	-	H	H	NO_2	H	> 100	> 100	> 100
13	CH_3	-	H	H	OCH_3	H	> 100	25.9 (17.7-38.0)	13.6 (12.3-15.2)
14	CH_3	-	H	OCH_3	OCH_3	OCH_3	> 60	32.9 (20.5-53.0)	9.82 (7.90-12.2)
15	CH_3	-	H	OH	OH	OH	14.7 (8.74-24.6)	> 100	14.3 (7.79-26.4)

16	OCH_3	-	H	H	NO_2	H	> 100	59.1 (57.1-61.2)	8.02 (6.90-9.32)
17	OCH_3	-	H	H	OCH_3	H	> 100	> 100	5.06 (3.89-6.57)
18	$OCOCH_3$	H	H	H	H	H	6.93 (5.76-8.33)	35.7 (27.9-45.8)	6.86 (5.86-8.03)
19	$OCOCH_3$	$OCOCH_3$	H	H	H	H	8.56 (6.90-10.6)	21.1 (16.6-26.8)	5.17 (4.85-5.50)
20	$OCOCH_3$	$OCOCH_3$	H	H	$OCOCH_3$	H	> 100	> 100	6.14 (3.24-11.6)
21	$OCOCH_3$	H	H	$OCOCH_3$	$OCOCH_3$	H	> 100	64.4 (49.0-84.6)	22.0 (12.5-38.7)
22	$OCOCH_3$	$OCOCH_3$	H	$OCOCH_3$	$OCOCH_3$	H	> 100	> 100	23.4 (14.5-37.9)
23	OH	H	H	H	H	H	4.62 (4.24-5.04)	42.3 (36.5-49.1)	5.09 (3.40-7.60)
24	OH	OH	H	H	H	H	2.40 (1.95-2.95)	12.1 (9.69-15.2)	3.85 (3.04-4.89)
25	OH	OH	H	H	OH	H	12.5 (10.3-15.4)	55.3 (45.3-67.4)	9.16 (7.12-11.8)
26	OH	H	H	OH	OH	H	6.20 (5.11-7.53)	14.0 (10.1-19.5)	23.6 (16.8-33.2)
27	OH	OH	H	OH	OH	H	6.28 (5.26-7.49)	25.5 (21.2-30.5)	8.50 (7.47-9.67)
Theophylline			-				6.77 (4.07-11.3)	1.71 (1.02-2.90)	86.4 (73.6-101)

Values are geometric means of three experiments and are given in µM with 95% confidence intervals. Numbers in parentheses are the numerical value of the standard uncertainty.

Based on previous results from our group, and on the potent A_3 receptor affinity of some of the described compounds,[21] a novel series of coumarin derivatives was investigated. Their common framework represented by an aryl group at position 3 and a substitution pattern at positions 7 and/or 8 was studied for their ability to modulate the affinity for

adenosine receptor subtypes. Different substituents were attached to the phenyl ring at position 3, based on their physicochemical properties. Substituents from different quadrants of the Craig plot were explored. In addition, the substitution by alkyl or alkoxy groups was studied. Finally, the difference between the presence of acetoxy and/or hydroxy groups linked to positions 7 and/or 8 of the coumarin scaffold was explored in detail. The effect of these substitutions on the affinity and selectivity for the four adenosine receptors was studied and compared. From our analysis, none of the derivatives showed measurable affinity for the A_{2B} receptor (K_i > 30 μM, data not shown).

The structural variety on the studied series allowed us to obtain different affinity profiles for the analyzed adenosine receptors. Selective A_3 ligands, A_{2A}/A_3 or A_1/A_3 dual ligands or non-selective ($A_1/A_{2A}/A_3$) ligands were obtained. The analysis of the results allowed us to have a detailed perspective on structure-activity relationships. In general, compounds with no substitutions on the 3-phenyl ring are not selective, presenting affinity for the three adenosine receptors (compounds **1**, **10**, **18**, **19**, **23** and **24**). This profile is independent of the nature of the 8 substitution (ethoxy, methyl, acetoxy) or even with substitutions at both 7 and 8 positions (compound **19**). These results are accordant with those obtained in our previous study.[21] 8-(2-Oxopropoxy)-3-phenylcoumarin (Figure 1A) has affinity for the three adenosine receptors in the low micromolar range (K_i A_1 = 10.4 μM, K_i A_{2A} = 16.1 μM and K_i A_3 = 7.1 μM).[21] In the present study, compound **24** shows similar affinity for the three adenosine receptors (K_i A_1 = 2.4 μM, K_i A_{2A} = 12.1 μM and K_i A_3 = 3.9 μM). In addition, compound **24** proved to be a better adenosine receptor ligand than theophylline, our reference compound, which is in clinical use to prevent and treat respiratory dysfunctions caused by asthma, emphysema, chronic bronchitis, and other lung diseases.[30] Besides being an A_{2B} receptor antagonist, theophylline is also a non-selective phosphodiesterase inhibitor. The profile of our

$A_1/A_{2A}/A_3$ compounds may be very interesting thinking about multifactorial conditions, as lung ischemia-reperfusion injury, likewise some xanthines, typical adenosine ligands.

When the scaffold presents a substituent at position 8 and another one at the *para* position of the 3-aryl ring, independently of the nature of the substituent at positions 8 (ethoxy, hydroxy, methyl or methoxy) or 3 (*p*-methylphenyl, *p*-bromophenyl or *p*-methoxyphenyl), the compounds tend to be potent and selective A_3 ligands (compounds **2**, **4**, **11** and **17**). This data expands our previously results.[21] The nanomolar affinity of compound **4** for the *h*A_3 receptor is about 2.5 times higher than that of our earlier reported 8-(2-oxopropoxy)-3-(*p*-tolyl)coumarin (Figure 1A).[21] So far, this is the best compound from all our research on the potential of coumarins as adenosine receptor ligands. In both cases, position 8 presents electron donating groups. This characteristic can be important to increase the activity and A_3 selectivity. In addition, it seems that the size of the substituent at position 8 plays an important role on the activity as well.

Another relevant structure-activity relationship was observed for the series presenting 2- or 3-substitutions at the 3-aryl ring (*meta* and *para* positions). Compounds **13**, **14** and **21** have affinity for both A_{2A} and A_3 receptors, and compound **15** has affinity for A_1 and A_3 receptors. The only example of a di-substituted compound at *ortho*/*para* positions (compound **8**), proved to be A_3 receptor selective (K_i A_3 = 16.6 μM).

Finally, the inclusion of substituents at both 7 and 8 positions of the coumarin ring (both acetoxy and hydroxy groups), independently of the substituents on the 3-aryl ring, tend to give potent non-selective ligands (compounds **19**, **24**, **25** and **27**). All these compounds have affinity for the A_1, A_{2A} and A_3 adenosine receptors in the low micromolar range. Compounds **20** and **22** are the exception, being selective for the A_3 receptor.

Finally, our most active and selective hA_3 compounds were functionally tested using a biosensor technology called GloSensor cAMP assay.[31] The detailed methodology is

described in the experimental section, and the binding data is shown in Table 2.

Table 2. *In vitro* antagonist activities of compounds **2**, **4**, **5** and **17** at the hA3 adenosine receptor.

Compound	hA3 (IC_{50} μM)
2	18.4 (10.5-26.2)
4	3.1 (1.7-4.5)
5	29.5 (17.7-41.2)
17	25.3 (15.5-31.1)

The values are given in μM with 95% confidence intervals in parentheses.

Cell-based functional assays showed that compounds **2**, **4**, **5** and **17** behave as hA3 receptor antagonists, being able to counteract NECA-inhibited cAMP accumulation.

In a homogeneous family of twenty-seven compounds, it can be clearly observed a pattern of affinity based on the structures (positions and nature of the substituents) that allows new structure-affinity relationship understanding. This can be useful for design of new potent and selective adenosine antagonists.

Molecular docking

We studied the most active compound in the series using molecular docking simulations in the hA3 receptor to establish the key residues and important interactions between the ligand and the protein. The protein structure of the hA3 was generated through homology modeling in previous studies by our research group[21,32] (general details are described in

Methods). We docked compound **4** to the hA3 with Glide standard precision (SP).[33] We followed a similar protocol already described in previous studies[21,32] and validated it in the hA2A protein for which there are some crystal structures available in the PDB. As an example, the root mean square deviation (RMSD) between theoretical and co-crystallized conformations of the ligands in the 3EML[34] and 3UZC crystal structures[35] was 0.69 and 1.90 respectively.[21]

Molecular docking simulations showed a binding mode for compound **4** in the hA3 pocket that pointed the 3-aryl ring towards the bottom of the cavity and the benzene of the coumarin towards the surface of the pocket. Compound **4** showed a pose in the hA3 that presented some resemblance with the co-crystallized ligands ZM241385 and T4E in the 3EML and 3UZC hA2A crystal structures (see Figure 3A). The hydroxyl substituent at position 8 along with the carbonyl group of the coumarin are hypothesized to play an important role in the anchoring with the protein and established two hydrogen bonds with the amide moiety of the residue Asn250 (see Figure 3B). The equivalent residue in the hA2A (Asn253) showed also an important role in ligand interaction in crystallographic and mutagenesis studies.[34,35,36] The benzopyrone moiety is proposed to establish aromatic π−π stacking interactions with the residue Phe168 of the second extracellular loop.

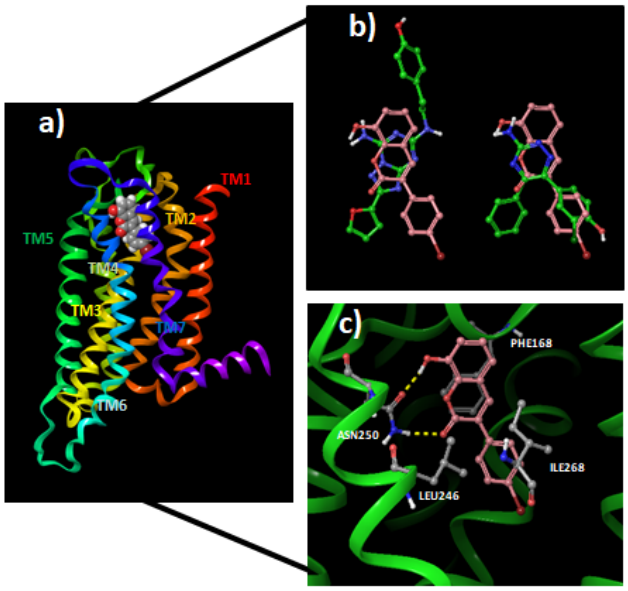

Figure 3. a) General view of the hA3 receptor bound to compound **4**. **b)** Comparison of the co-crystallized conformations for the compounds (green carbons) in the hA2A [3EML (left) and 3UZC (right)] with the binding mode extracted from docking in hA3 for compound **4** (pink carbons). Both proteins, hA2A and hA3, were superimposed. **c)** Hypothetical binding mode in the hA3 determined for compound **4** along with important residues in ligand recognition. Hydrogen bonds are represented in yellow color. Ribbons in the protein were partially omitted for clarity.

We extended the ligand-protein interaction analysis to per residue energy contributions (see Figure 4A). The energy is calculated as a sum of different contributions considering Coulomb, *van der Waals* and H-bond energies. Residues Asn250, Phe168, Ile268, Leu246, Leu264 and Leu90 have the highest contribution in the ligand-protein recognition. Hydroxyl group at position 8 of the coumarin played an important role for the interaction with residue Asn250 and it could be a key factor to explain the high activity shown by compound **4**. The bromine substituent at *para* position of the 3-aryl ring could

be also a suitable substituent for the protein interaction. Compound **23**, structurally similar to compound **4** but with no substitution in the 3-aryl ring showed a similar binding mode, but with lower Coulomb/*van der Waals* contributions with the residues close to the 3-aryl (see Figure 4B). The bromine substituent caused a slight increase in the interaction with residues Leu90, Ser271 and His272 compared to the 3-aryl ring without substituent (compound **23**). Moreover, we calculated the favored hydrophobic and hydrophilic areas inside the hA_3 protein pocket. The surfaces were generated taking into account the residues located in a radius of 5Å from the ligand. Hydroxyl group at position 8 and the oxygen atoms of the pyrone ring are placed in polar areas whereas the coumarin and the 3-aryl scaffold are placed in a hydrophobic region (see Figure 4C). The bromine atom is buried in a deep hydrophobic area that can favor the interaction with the protein. In fact, besides hydrophobic interactions with residues Trp243 and Leu90 (also shown by compound **23**) we detected additional hydrophobic interactions with residues Val65 and Val61. Our proposed binding mode explains the ability of compound **4** to bind the hA_3 receptor with high affinity. Our results agree with previous studies focused on adenosine receptors[21,32,34-37] in which residues such as Asn250 and Phe168 were also found to be important in ligand-protein recognition.

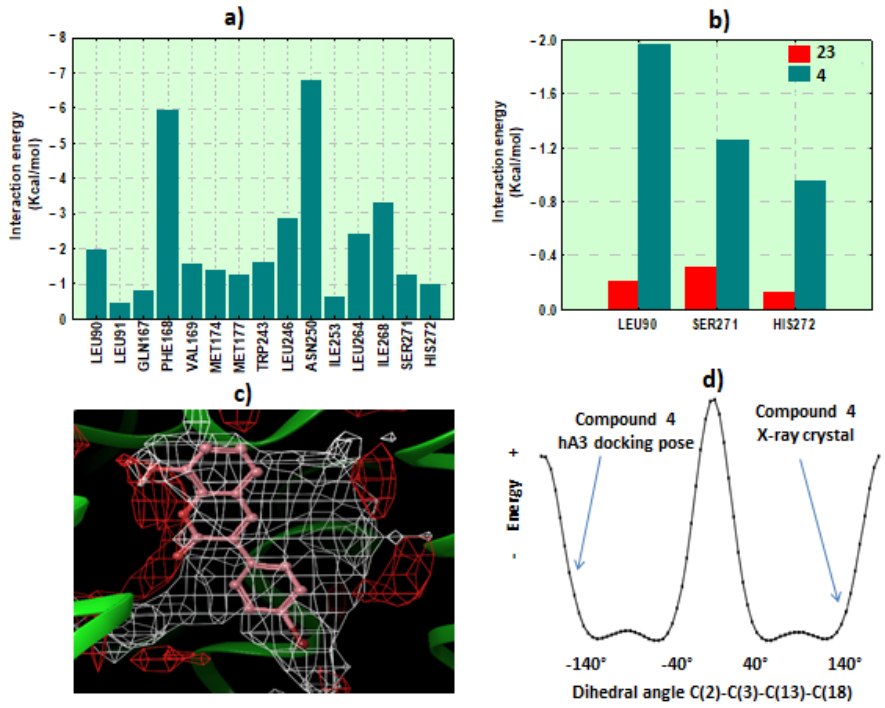

Figure 4. **a)** Residue contribution to the interaction with ligand **4** (sum of Coulomb, *van der Waals* and hydrogen bond energies). **b)** Differences in the residue contribution in compound **4** and compound **23**. Bromine substitution in the 3-aryl ring (compound **4**) causes a higher Coulomb/*van der Waals* contribution in nearby residues. **c)** Hydrophobic (white) and hydrophilic (red) areas inside the hA_3 with the binding mode detected for compound **4** (isovalues of -0.5 and -4.87 for hydrophobic and hydrophilic surfaces respectively). The 8-hydroxyl group is placed in the hydrophilic region whereas the 3-aryl scaffold is placed in the hydrophobic area. **d)** Dihedral angle energy plot for compound **4** extracted from conformational analysis.

The results provided by the docking calculations are in strong agreement with the X-ray structure of compound **4** (RMSD=0.16Å). As the analysis of the conformational preorganization of the compound could provide some insights in drug design,[38] we

performed a comparative structural study in terms of energetic stabilization around the dihedral angle C(2)-C(3)-C(13)-C(18) between the 3-aryl ring and the coumarin scaffold in compound **4**. The dihedral angle was rotated in 5-degree increments during the conformational analysis. Compound **4** showed two optimal energetic areas with values for the dihedral angle from -140° to -40° and from 40° to 140°. The described X-ray crystallized structure and the docking pose showed values of 145.4° and -152.1° for the dihedral angle. It has been reported that in many cases the bioactive ligand conformation is not correspondent with the global minimum energy conformer as both protein and ligand can reorganize their atomic coordinates to optimize complementarity.[39] For compound **4**, the X-ray and the docking conformation are close to the global minimum energy structure. The dihedral angle energy plot for compound **4** is shown in Figure 4D with the values obtained in docking and X-ray studies.

Compound **4** showed hA_3 activity and no affinity for the other adenosine subtypes. We performed additional molecular docking simulations in the hA_{2A} crystallized structure 3EML to explain the affinity decrease for compound **4**. Molecular docking with no crystallographic water in the hA_{2A} pocket yielded a binding mode deeply buried in the cavity (see Figure 5A). The described pose would need to shift different crystallized water molecules that establish a stabilizing hydrogen bonding network with the residues. This fact could have an important impact in ligand binding affinity and enthalpy/entropy of the system.[40] The global process could be energetically unfavorable reducing the activity of compound **4** in hA_{2A}. Nevertheless, the docking with crystallographic water molecules in the hA_{2A} cavity showed a pose for compound **4** that binds a shallower area of the pocket and disrupts key interactions with some residues located deeper in the cavity, such as Asn253 (see Figure 5B). The disruption of the binding mode explained for compound **4** in the hA_3 could be responsible for the low activity detected in hA_{2A}. In fact, compound

4 showed a different residue profile binding in the hA_3 and hA_{2A} with a clear reduction in the interaction energy between the ligand and Asn253, a key residue in the interaction between compound **4** and the hA_3 (see Supporting Information).

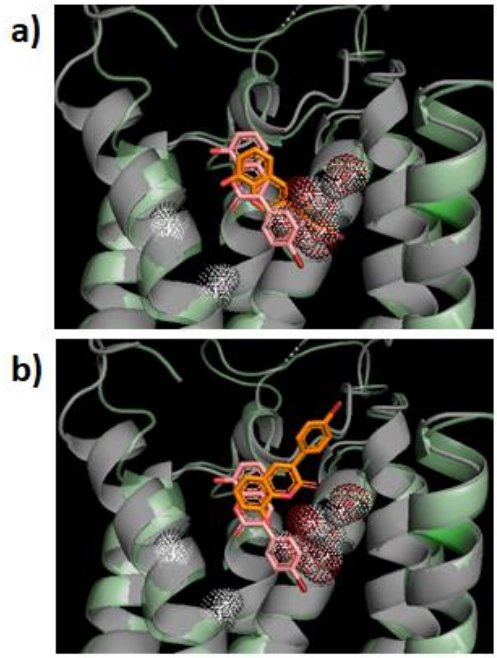

Figure 5. Superposition of the binding modes for compound **4** extracted from docking in hA_3 (ligand in pink carbons) and hA_{2A} (ligand in orange carbons). **a)** Hypothetical binding mode for compound **4** buried in an area of multiple crystallographic water molecules in the hA_{2A} (although water molecules are shown in red/white mesh, the docking was performed with no water in the cavity). This hypothetical pose would need to displace the mentioned waters. **b)** Hypothetical binding mode for compound **4** in a shallower area close to the extracellular loops in the hA_{2A} (docking performed with water molecules in the pocket). Disruption of the hypothetical binding mode detected for compound **4** in hA_3 (pink carbons) could be the cause of lack of affinity in the hA_{2A}.

Some of the residues located in the extracellular domain of the hA_3 are not present in the other subtypes, which can be also an important factor to explain the selectivity. Residues such as Gln167 with polar properties, Val169 and Leu264 with hydrophobic characteristics are substituted in the hA_{2A} by the corresponding hydrophobic Leu167, the negative charged and hydrophilic Glu169 and hydrophobic Met270. The subtype hA_1 also contains some residues, such as Glu170, Glu172 and Thr270 with hydrophilic properties more suitable for the interaction with polar substituents. The chemical characteristics of the different residues can affect the entrance of the ligand in the pocket as well as the accommodation in the binding cleft and favor the selectivity against the hA_3.

Conclusions

3-Arylcoumarins proved to be an interesting scaffold for the design of multitarget molecules. In particular, 8-substituted compounds are promising molecules as novel adenosine receptor antagonists, presenting different affinity and selectivity profiles. An extensive analysis of the results allowed to conclude that the affinity and/or selectivity of the coumarins towards adenosine receptors can be modulated by the nature of the substituents attached at positions 3, 7 and 8 of the coumarin scaffold. Compound **4** (3-(4-bromophenyl)-8-hydroxycoumarin) proved to be the best compound of the studied series, and all the molecules studied by our group so far. Its structure was corroborated by X-ray crystallography, revealing that this coumarin derivative presents a *p*-bromophenyl substituent at position 3 and a hydroxyl group at position 8. This last substituent played an important role for the interaction with the Asn250 residue and it could be a key factor to explain the high affinity shown by this antagonist. The substituents on the 3-aryl ring are also important for this selectivity pattern. On the other hand, compound **24** proved to be the compound with the highest affinity on three receptors, being a better ligand than

the reference compound, theophylline. This series offers the possibility to better understand important clues to modulate the interactions with adenosine receptors. Compound **24** can be the inspiration for the design of multifunctional compounds with interest on multifactorial conditions, and compound **4** can be the inspiration for the design and synthesis of new coumarins as potent and selective A_3 antagonists.

EXPERIMENTAL SECTION

CHEMISTRY

General remarks. Starting materials and reagents were obtained from commercial suppliers (Sigma-Aldrich) and were used without further purification. Melting points (Mp) are uncorrected and were determined with a Reichert Kofler thermopan or in capillary tubes in a Büchi 510 apparatus. ^{1}H NMR (300 MHz) and ^{13}C NMR (75.4 MHz) spectra were recorded with a Bruker AMX spectrometer using $CDCl_3$ or DMSO-d_6 as solvent. Chemical shifts (δ) are expressed in parts per million (ppm) using TMS as an internal standard. Coupling constants *J* are expressed in Hertz (Hz). Spin multiplicities are given as s (singlet), d (doublet), t (triplet), q (quartet) and m (multiplet). Mass spectrometry was carried out with a Hewlett-Packard 5988A spectrometer. Elemental analyses were performed by a Perkin-Elmer 240B microanalyzer and are within ±0.4% of calculated values in all cases. The analytical results document ≥ 98% purity for all compounds. Flash chromatography (FC) was performed on silica gel (Merck 60, 230-400 mesh); analytical TLC was performed on precoated silica gel plates (Merck 60 F254). Organic solutions were dried over anhydrous sodium sulfate. Concentration and evaporation of the solvent after reaction or extraction was carried out on a rotary evaporator (Büchi Rotavapor) operating under reduced pressure.

General procedure for the synthesis of 3-phenylcoumarins (1-3, 5-14, 16 and 17). A solution of 2-hydroxybenzaldehyde (7.34 mmol) and the corresponding phenylacetic acid (9.18 mmol) in dimethyl sulfoxide (15 mL) was prepared. *N,N'*-Dicyclohexylcarbodiimide (11.46 mmol) was added, and the mixture was heated in an oil bath at 110 ºC for 24 h. Ice (100 mL) and acetic acid (10 mL) were added to the reaction mixture. After keeping it at room temperature for 2 h, the mixture was extracted with ether (3 x 25 mL). The organic layer was extracted with sodium bicarbonate solution (50 mL, 5%) and then water (20 mL). The solvent was evaporated under vacuum, and the dry residue was purified by FC (hexane/ethyl acetate 9:1).

3-(4-bromophenyl)-8-ethoxycoumarin (compound 3). Yield 41%. M.p. 162-163 ºC. ^{1}H NMR ($CDCl_3$) δ (ppm), *J* (Hz): 1.52 (t, 3H, CH_3, *J*=7.0), 4.20 (q, 2H, CH_2, *J*=7.0), 7.06-7.24 (m, 3H, H-5, H-6, H-7), 7.32-7.45 (m, 4H, H-2', H-3', H-5', H-6'), 7.79 (s, 1H, H-4). ^{13}C NMR ($CDCl_3$) δ (ppm): 14.8, 65.0, 114.7, 119.3, 120.2, 123.14 124.5, 127.3, 130.1, 131.6, 133.6, 140.2, 143.4, 146.4, 159.9. MS *m/z* (%): 347 (18), 346 (98), 345 (19), 344 (M^+, 100). Ana. Elem. Calc. for $C_{17}H_{13}BrO_3$: C, 59.15; H, 3.80. Found: C 58.98, H 3.80.

8-ethoxy-3-(3,4-dimethoxyphenyl)coumarin (compound 7). Yield 41%. M.p. 138-139 ºC. ^{1}H NMR ($CDCl_3$) δ (ppm), *J* (Hz): 1.53 (t, 3H, CH_3, *J*=7.0), 3.90 (s, 3H, OCH_3), 3.95 (s, 3H, OCH_3), 4.21 (q, 2H, CH_2, *J*=7.0), 6.94 (d, 1H, H-7, *J*=8.2), 7.02-7.09 (m, 2H, H-2', H-6'), 7.20 (d, 1H, H-5', *J*=7.9), 7.28-7.33 (m, 2H, H-5, H-6), 7.77 (s, 1H, H-4). ^{13}C NMR ($CDCl_3$) δ (ppm): 14.5, 55.7, 64.6, 110.7, 111.5, 114.0, 118.9, 120.2, 121.0, 124.0, 127.1, 128.0, 138.7, 142.8, 146.0, 148.4, 149.4, 160.1. MS *m/z* (%): 327 (55), 326 (M^+, 100). Anal. Elem. Calc. for $C_{19}H_{18}O_5$: C, 69.93; H, 5.56. Found: C, 69.91; H, 5.53.

8-ethoxy-3-(2,4-dimethoxyphenyl)coumarin (compound 8). Yield 36%. M.p. 95-96 ºC. ^{1}H NMR ($CDCl_3$) δ (ppm), *J* (Hz): 1.50 (t, 3H, CH_3, *J*=7.0), 3.80 (s, 3H, OCH_3), 3.82

(s, 3H, OCH_3), 4.19 (q, 2H, CH_2, *J*=7.0), 6.45-6.57 (m, 2H, H-3', H-5'), 7.03-7.09 (m, 1H, H-7), 7.14-7.19 (m, 2H, H-6, H-5), 7.30 (d, 1H, H-6', *J*=8.9), 7.68 (s, 1H, H-4). ^{13}C NMR ($CDCl_3$) δ (ppm): 14.8, 55.4, 55.7, 64.9, 99.0, 104.5, 114.1, 116.8, 119.1, 120.4, 124.0, 126.3, 131.4, 141.4, 146.3, 154.2, 158.3, 160.2, 161.4. MS *m/z* (%): 327 (12), 326 (M^+, 47). Anal. Elem. Calc. for $C_{19}H_{18}O_5$: C, 69.93; H, 5.56. Found: C, 69.96; H, 5.58.

8-ethoxy-3-(3,4,5-trimethoxyphenyl)coumarin (compound 9). Yield 40%. M.p. 142-143 ºC. ^1H NMR ($CDCl_3$) δ (ppm), *J* (Hz): 1.58 (t, 3H, CH_3, *J*=7.0), 3.94 (s, 3H, OCH_3), 3.96 (s, 3H, OCH_3), 3.99 (s, 3H, OCH_3), 4.25 (q, 2H, CH_2, *J*=7.0), 7.0 (s, 2H, H-2', H-6'), 7.14-7.20 (m, 1H, H-6), 7.24-7.27 (m, 1H, H-7), 7.30-7.32 (m, 1H, H-5), 7.83 (s, 1H, H-4). ^{13}C NMR ($CDCl_3$) δ (ppm): 14.8, 56.2, 56.3, 65.0, 105.9, 114.5, 119.2, 120.3, 124.4, 128.2, 130.2, 139.7, 133.8, 146.3, 153.0. MS *m/z* (%): 357 (23), 356 (M^+, 100). Anal. Elem. Calc. for $C_{20}H_{20}O_6$: C, 67.41; H, 5.66. Found: C, 67.42; H, 5.68.

8-methyl-3-(4-nitrophenyl)coumarin (compound 12). Yield 61%. M.p. 229-230 ºC. ^1H NMR (DMSO-d_6) δ (ppm), *J* (Hz): 2.38 (s, 3H, CH_3), 7.28 (t, 1H, H-6, *J*=7.4), 7.52 (d, 1H, H-7, *J*=7.4), 7.61 (d, 1H, H-5, *J*=7.4), 7.99 (d, 2H, H-2', H-6', *J*=9.0), 8.28 (d, 2H, H-3', H-5', *J*=9.0), 8.41 (s, 1H, H-4). ^{13}C NMR (DMSO-d_6) δ (ppm): 15.3, 123.8, 124.8, 124.9, 125.4, 127.3, 130.2, 131.3, 134.1, 141.8, 143.4, 147.5, 152.0, 159.8. MS *m/z* (%): 282 (18), 281 (M^+, 100). Anal. Elem. Calc. for $C_{16}H_{11}NO_4$: C, 68.33; H, 3.94. Found: C, 68.36; H, 3.93.

3-(3,4-dimethoxyphenyl)-8-methylcoumarin (compound 13). Yield 63%. M.p. 135-136 ºC. ^1H NMR ($CDCl_3$) δ (ppm), *J* (Hz): 2.51 (s, 3H, CH_3), 3.94 (s, 6H, 2xOCH_3), 6.95 (d, 1H, H-5', *J*=8.1), 7.16-7.39 (m, 5H, H-5, H-6, H-7, H-2', H-6'), 7.77 (s, 1H, H-4). ^{13}C NMR ($CDCl_3$) δ (ppm): 15.4, 55.9, 110.9, 111.7, 119.4, 121.1, 124.0, 125.4, 125.8, 127.5, 127.5, 132.4, 139.2, 148.6, 149.6, 151.6, 160.9. MS *m/z* (%): 297 (46), 296 (M^+, 100). Anal. Elem. Calc. for $C_{18}H_{16}O_4$: C, 72.96; H, 5.44. Found: C, 73.00; H, 5.49.

3-(3,4,5-trimethoxyphenyl)-8-methylcoumarin (compound 14). Yield 69%. M.p. 163-164 ºC. ^{1}H NMR ($CDCl_3$) δ (ppm), *J* (Hz): 2.49 (s, 3H, CH_3), 3.89 (s, 3H, OCH_3), 3.90 (s, 3H, OCH_3), 3.93 (s, 3H, OCH_3), 6.95 (s, 2H, H-2', H-6'), 7.18-7.23 (m, 2H, H-6, H-7), 7.38 (d, 1H, H-5, *J*=7.4), 7.79 (s, 1H, H-4). ^{13}C NMR ($CDCl_3$) δ (ppm): 15.4, 56.2, 56.3, 106.0, 119.3, 124.1, 125.6, 125.9, 127.7, 130.3, 132.7, 138.7, 139.9, 151.7, 153.1, 160.7. MS *m/z* (%): 327 (23), 326 (M^+, 100). Ana. Elem. Calc. for $C_{19}H_{18}O_5$: C, 69.93; H, 5.56. Found: C, 69.96; H, 5.59.

General procedure for the synthesis of hydroxy-3-phenylcoumarins (4 and 15). A solution of **3** or **14** (0.50 mmol) in acetic acid (5 mL) and acetic anhydride (5 mL), at 0 ºC, was prepared. Hydriodic acid 57% (10 mL) was added dropwise. The mixture was stirred, under reflux temperature, for 3 h. The solvent was evaporated under vacuum, and the dry residue was purified by crystallization (CH_3CN).

3-(4-bromophenyl)-8-hydroxycoumarin (compound 4). Yield 42%. M.p. 261-217 ºC. ^{1}H NMR (DMSO-*d*$_6$) δ (ppm), *J* (Hz): 7.05-7.16 (m, 3H, H-5, H-6, H-7), 7.56-7.71 (m, 4H, H-2', H-3', H-5', H-6'), 8.22 (s, 1H, H-4), 10.27 (s, 1H, OH). ^{13}C NMR (DMSO-*d*$_6$) δ (ppm): 118.2, 118.7, 120.3, 121.9, 124.6, 125.5, 130.6, 131.2, 133.9, 141.3, 141.7, 144.4, 159.5. MS *m/z* (%): 319 (16), 318 (98), 317 (17), 316 (M^+, 100). Ana. Elem. Calc. for $C_{15}H_9BrO_3$: C, 56.81; H, 2.86. Found: C 56.84, H 2.87.

General procedure for the synthesis of acetoxy-3-phenylcoumarins (18-22). Compound **18-22** were synthesized under anhydrous conditions, using material previously dried at 60 ºC for at least 12 h and at 300 ºC during few minutes immediately before use. A solution containing anhydrous CH_3CO_2K (2.94 mmol), phenylacetic acid (1.67 mmol) and the corresponding hydroxysalicylaldehyde (1.67 mmol), in Ac_2O (1.2

mL), was refluxed for 16 h. The reaction mixture was cooled, neutralized with 10% aqueous $NaHCO_3$, and extracted with EtOAc (3 x 30 mL). The organic layers were combined, washed with distilled water, dried (anhydrous Na_2SO_4), and evaporated under reduced pressure. The product was purified by recrystallization in EtOH and dried, to afford the desired compound.

8-acetoxy-3-phenylcoumarin (compound 18). Yield 64%. M.p. 189-190 ºC. ^{1}H NMR ($CDCl_3$) δ (ppm), *J* (Hz): 2.44 (s, 3H, CH_3), 7.18-7.50 (m, 7H, H-2', H-3', H-4', H-5', H-6', H-6, H-7), 7.66-7.71 (m, 1H, H-5), 7.83 (s, 1H, H-4). ^{13}C NMR ($CDCl_3$) δ (ppm): 20.7, 119.3, 123.0, 124.5, 124.8, 126.0, 128.2, 128.9, 129.2, 135.3, 142.1, 144.2, 149.2, 160.9, 168.5. MS *m/z* (%): 281 (19), 280 (M^+, 100). Ana. Elem. Calc. for $C_{17}H_{12}O_4$: C, 72.85; H, 4.32. Found: C, 72.90; H, 4.30.

7,8-diacetoxy-3-phenylcoumarin (compound 19). Yield 81%. M.p. 171-172 ºC. ^{1}H NMR ($CDCl_3$) δ (ppm), *J* (Hz): 2.34 (s, 3H, CH_3), 2.43 (s, 3H, CH_3), 7.15 (d, 1H, H-6, *J*=8.7), 7.39-7.49 (m, 4H, H-5, H-2', H-4', H-6'), 7.64-7.69 (m 2H, H-3', H-5'), 7.78 (s, 1H, H-4). ^{13}C NMR ($CDCl_3$) δ (ppm): 20.3, 20.6, 118.5, 119.1, 124.9, 128.1, 128.5, 129.0, 130.0, 134.3, 139.1, 144.9, 146.5, 159.0, 167.4, 167.8. MS *m/z* (%): 339 (11), 338 (M^+, 100). Ana. Elem. Calc. for $C_{19}H_{14}O_6$: C, 67.45; H, 4.17. Found: C, 67.52; H, 4.20.

7,8-diacetoxy-3-(4-acetoxyphenyl)coumarin (compound 20). Yield 75%. M.p. 195-196 ºC. ^{1}H NMR ($CDCl_3$) δ (ppm), *J* (Hz): 2.32 (s, 3H, CH_3), 2.34 (s, 3H, CH_3), 2.42 (s, 3H, CH_3), 7.13-7.19 (m, 3H, H-6, H-3', H-5'), 7.41 (d, 1H, H-5, *J*=8.7), 7.68 (d, 2H, H-2', H-6', *J*=8.6), 7.77 (s, 1H, H-4). ^{13}C NMR ($CDCl_3$) δ (ppm): 20.2, 20.5, 21.1, 118.3, 119.1, 121.6, 124.9, 127.1, 129.6, 131.8, 131.9, 139.1, 144.2, 144.92, 151.1, 161.9, 167.3. MS *m/z* (%): 397 (9), 396 (M^+, 93). Ana. Elem. Calc. for $C_{21}H_{16}O_8$: C, 63.64; H, 4.07. Found: C, 63.61; H, 4.09.

8-acetoxy-3-(3,4-diacetoxyphenyl)coumarin (compound 21). Yield 47%. M.p. 144-145 ºC. ^{1}H NMR ($CDCl_3$) δ (ppm), *J* (Hz): 2.33 (s, 6H, 2xCH_3), 2.44 (s, 3H, CH_3), 7.27-7.31 (m, 3H, H-5', H-2', H-6), 7.41-7.45 (m, 1H, H-7), 7.58-7.64 (m, 2H, H-6', H-5), 7.84 (s, 1H, H-4). ^{13}C NMR ($CDCl_3$) δ (ppm): 20.6, 20.6, 20.6, 120.6, 123.4, 123.6, 124.3, 125.1, 125.4, 126.6, 127.0, 132.8, 137.5, 139.8, 139.9, 140.0, 141.9, 158.8, 168.0, 168.1, 168.5. MS *m/z* (%): 397 (15), 396 (M^+, 89). Ana. Elem. Calc. for $C_{21}H_{16}O_8$: C, 63.64; H, 4.07. Found: C, 63.66; H, 4.10.

7,8-diacetoxy-3-(3,4-diacetoxyphenyl)coumarin (compound 22). Yield 54%. M.p. 202-203 ºC. ^{1}H NMR ($CDCl_3$) δ (ppm), *J* (Hz): 2.35 (s, 3H, CH_3), 2.37 (s, 3H, CH_3), 2.39 (s, 3H, CH_3), 2.46 (s, 3H, CH_3), 7.20 (d, 1H, H-6', *J*=8.6), 7.30 (s, 1H, H-2'), 7.46 (d, 1H, H-5', *J*=8.6), 7.59-7.65 (m, 2H, H-5, H-6), 7.84 (s, 1H, H-4). ^{13}C NMR ($CDCl_3$) δ (ppm): 20.1, 20.2, 20.5, 20.6, 118.1, 119.2, 122.0, 123.4, 123.6, 125.9, 126.2, 132.7, 139.5, 141.9, 142.6, 145.1, 148.9, 150.3, 160.4, 167.6. MS *m/z* (%): 455 (9), 454 (M^+, 92). Ana. Elem. Calc. for $C_{23}H_{18}O_{10}$: C, 60.80; H, 3.99. Found: C, 60.82; H, 4.01.

General procedure for the synthesis of hydroxy-3-phenylcoumarins (23-27). Compounds **23-27** were obtained by hydrolysis of their acetoxylated counterparts **18-22**, respectively. The appropriate acetoxylated coumarin, mixed with 2N aqueous HCl and MeOH, was refluxed during 3 h. The resulting reaction mixture was cooled in an ice-bath and the reaction product, obtained as solid, was filtered, washed with cold distilled water, and dried under vacuum, to afford the desired compound.

7,8-dihydroxy-3-(4-hydroxyphenyl)coumarin (compound 25). Yield 91%. M.p. 290-291 ºC. ^{1}H NMR (DMSO-*d*$_6$) δ (ppm), *J* (Hz): 6.78-6.81 (m, 3H, H-6, H-3', H-5'), 7.04 (d, 1H, H-5, *J*=8.5), 7.51-7.55 (m, 2H, H-2', H-6'), 7.97 (s, 1H, H-4), 9.63 (s, 1H, OH), 10.05 (s, 1H, OH), 10.08 (s, 1H, OH). ^{13}C NMR (DMSO-*d*$_6$) δ (ppm): 115.0, 115.2, 116.3,

126.0, 126.6, 129.8, 133.6, 139.7, 142.5, 149.0, 149.3, 157.2, 162.7. MS *m/z* (%): 271 (16), 270 (M^+, 100). Ana. Elem. Calc. for $C_{15}H_{10}O_5$: C, 66.67; H, 3.73. Found: C, 66.65; H, 3.75.

8-hydroxy-3-(3,4-dihydroxyphenyl)coumarin (compound 26). Yield 79%. M.p. 259-260 ºC. ^{1}H NMR (DMSO-*d6*) δ (ppm), *J* (Hz): 7.79 (d, 1H, H-5', *J*=8.3), 7.01-7.22 (m, 5H, H-5, H-6, H-7, H-2', H-6'), 8.03 (s, 1H, H-4), 9.07 (s, 1H, OH), 9.22 (s, 1H, OH), 10.16 (s, 1H, OH). ^{13}C NMR (DMSO-*d6*) δ (ppm): 115.5, 116.2, 117.6, 118.5, 120.0, 120.8, 124.6, 125.9, 126.8, 138.8, 139.0, 145.0, 146.3, 155.2, 164.8. MS *m/z* (%): 271 (18), 270 (M^+, 100). Ana. Elem. Calc. for $C_{15}H_{10}O_5$: C, 66.67; H, 3.73. Found: C, 66.66; H, 3.71.

Compounds 1, **2**, **5**, **6**, **10**, **11**, **15**, **16**, **17**, **23**, **24** and **27** have been previously described.[23,24,25,41,42,43,44,45,46]

Adenosine receptors affinity. The affinity of the studied compounds for the human adenosine receptor subtypes hA_1, hA_{2A} and hA_3, was determined with radioligand competition experiments in Chinese hamster ovary (CHO) cells that were stably transfected with the individual receptor subtypes. The radioligands used were 1 nM [^{3}H]CCPA for hA_1, 10 nM [^{3}H]NECA for hA_{2A}, and 1 nM [^{3}H]HEMADO for hA_3 receptors. The results were expressed as K_i values (dissociation constants), which were calculated with the program Prism (GraphPad Software). K_i values are reported as geometric means of three independent experiments with each tested concentration of compound measured in duplicate. As an interval estimate for the dissociation constants, 95% confidence intervals are given in parentheses. Details for pharmacological experiments are described in previous works.[26,29] Due to the lack of a suitable radioligand

for hA_{2B} receptors, the potency of antagonists at the hA_{2B} receptor (expressed on CHO cells) was determined by inhibition of NECA-stimulated adenylyl cyclase activity.

GloSensor cAMP Assay. Functional A_3 adenosine receptor activity was determined using a biosensor technology called GloSensor cAMP assay. It consists of a mutant form of Firefly luciferase into which a cAMP-binding protein moiety has been inserted. When the cAMP binds the biosensor there is a conformational change which induce an increase of light output that allow to evaluate the activity of ligands at the receptor under study. Briefly, cells stably expressing the hA_3 adenosine receptor and transiently the biosensor, were harvested and incubated in equilibration medium containing a 3% v/v GloSensor cAMP reagent stock solution, 10% FBS, and 87% CO_2 independent medium. After 2 h of incubation at room temperature, cells were dispensed in the wells of a 384-well plate and NECA reference agonist or the understudy compounds, at different concentrations, were added. When compounds were unable to inhibit the cAMP production they were studied as antagonists. In particular, the antagonist profile was evaluated by assessing the ability of these compounds to counteract NECA-induced decrease of cAMP accumulation. Responses were expressed as percentage of the maximal relative luminescence units (RLU). Concentration–response curves were fitted by a nonlinear regression with the Prism 5.0 programme (GraphPAD Software, San Diego, CA, USA). The antagonist profile of the compounds was expressed as IC_{50}, which is the concentration of antagonists that produces 50% inhibition of the agonist effect. Three independent experiments with each tested concentration of compound measured five times. The final values are given with 95% confidence intervals.[31]

hA$_3$ homology model. Homology model of hA$_3$ receptor along with a description of its construction was previously published by our group.[21,32] The hA$_{2A}$ crystallized structure (PDB code: 3EML)[34] was used as a template for the development of the homology model. The alignment between both proteins was reported previously and it is included in Katritch *et al.*,[47] considering highly conserved residues in the TMs. The Homology Model module in MOE software was used to develop the hA$_3$ model.[48] For residues that are identical, the heavy atoms coordinates are copied to the new target from the template, whereas only the backbone is taken into account for different residues. The residues placed in the loops with no specified coordinates are constructed based on high resolution fragments available in the PDB. A Boltzmann-weighted function is used for the selection of the loops. The top hA$_3$ model according to the Generalized Born/Volume Integral (GB/VI) scoring was selected. The geometrical quality of Phi-Psi dihedrals, bond lengths, bond angles, dihedrals, side chains and non-bonded interactions was assessed with the Protein Geometry module. Protein pocket was optimized by docking high affinity ligands using the Induced Fit Docking workflow allowing flexibility in the pocket residues.[33] The best hA$_3$ homology models showed ROC curves greater than 0.80 in the discrimination of ligands from decoys. A detailed description of the homology modeling was provided in previous studies.[21,32]

Moreover, our hA$_3$ receptor was compared to a model generated using the protein structure homology model server SwissModel.[49] The server automatically detected the hA$_1$ (PDB code: 5UEN)[50] as the best template and generated a hA$_3$ model that is in agreement with our reported homology model using as a template the hA$_{2A}$ receptor (PDB code: 3EML). The average RMSD between both models is 2.8 Å whereas the RMSD between both pockets is 0.9 Å. More details about homology model comparison are provided in the Supporting Information.

Molecular docking. Molecular docking simulations in the hA_3 and hA_{2A} proteins were run using the Schrödinger package.[33] Ligands were prepared with the LigPrep module that included the next steps: generation of tautomers and different protonation states (pH=7±2) and optimization of the molecular structures. Protein structures were also prepared with the module Protein Preparation Wizard to optimize protonation states of some residues and the H-bond network of the proteins. After this step, a grid centered in the pocket was generated (*van der Waals* radius scaling=1.0; partial charge cut-off=0.25). The ligands were docked to the hA_3 and hA_{2A} using Glide standard precision (SP mode). Top scoring function poses were selected as representative of the simulations.

ASSOCIATED CONTENT

* Supporting Information

The Supporting Information is available free of charge on the ACS Publications website at DOI: XXX.

AUTHOR INFORMATION

Corresponding Authors

* Maria J. Matos: phone, +34 881814936; E-mail, mariajoao.correiapinto@usc.es or maria.matos@fc.up.pt.

* Fernanda Borges: phone, +351 220402560; E-mail, fborges@fc.up.pt.

ORCID

Maria J. Matos: 0000-0002-3470-8299

S. Vilar: 0000-0003-2663-4370

S. Vazquez-Rodriguez: 0000-0003-1356-8984

K.-N. Klotz: 0000-0003-3553-3205

M. Buccioni: 0000-0002-8383-0813

G. Delogu: 0000-0003-0307-1544

L. Santana: 0000-0001-6056-8253

E. Uriarte: 0000-0001-6218-2899

F. Borges: 0000-0003-1050-2402

Author Contributions

M.J.M., E.U. and F.B. conceived and supervised the study. M.J.M., S.V.-R. and G.D. performed the synthesis, purification and characterization of the compounds. E.U. and L.S. co-supervised the synthetic part of the work. S.K. and M.B. performed the pharmacological assays on adenosine receptors. K.-N.K. supervised and validated the pharmacological assays. S.V. performed the docking studies. L.S. and F.B. co-supervised the modelling studies. M.J.M. wrote the manuscript with contributions from all authors. All authors approved the final version of the manuscript.

Notes

The authors declare no competing financial interest.

ACKNOWLEDGEMENTS

This work was partially supported by University of Porto and University of Santiago de Compostela. Authors would like to thank the use of RIAIDT-USC analytical facilities. This project has received funding from the European Union's Horizon 2020 research and innovation programme under the Marie Sklodowska-Curie grant agreement No 744389, supporting S.V.R. postdoctoral fellowship (TEDCIP). Authors would like to thank

Angeles Alvariño Plan Galego de Investigación, Innovación e Crecemento 2011–2015 (S.V.), European Social Fund, FCT, POPH, and QREN (SFRH/BPD/95345/2013, M.J.M.) for funding. This project has received funding from Xunta da Galicia and Galician Plan of Research, Innovation and Growth 2011–2015 (Plan I2C, ED481B 2014/086–0 and ED481B 2018/007, M.J.M.). This project was supported by Foundation for Science and Technology (FCT), and FEDER/COMPETE (POCI-01-0145-FEDER-006980).

ABBREVIATIONS USED

K_i, dissociation constant; GPCR, G protein-coupled receptors; DCC, *N,N'*-dicyclohexylcarbodiimide; Ac_2O, acetic anhydride; MeOH, methanol; AcOH, acetic acid; μM, micromolar; PDB, protein data bank; SP, Glide standard precision; RMSD, root mean square deviation; FC, flash chromatography; CHO cells, Chinese hamster ovary cells. [^{3}H]CCPA, (2R,3R,4S,5R)-2-(2-Chloro-6-cyclopentylamino-purin-9-yl)-5-hydroxymethyl-tetrahydro-3,4-diol); [^{3}H]NECA, (1-(6-amino-9*H*-purin-9-yl)-1-deoxy-*N*-ethyl-*β*-dribofuronamide); [^{3}H]HEMADO, 2-(1-hexynyl)-N_6-methyladenosine [3H]; MOE, molecular operating environment; GB, generalized born; VI, volume integral; ROC, receiver operating characteristic.

REFERENCES

1 Sheth, S.; Brito, R.; Mukherjea, D.; Rybak, L. P.; Ramkumar, V. Adenosine receptors: expression, function and regulation. *Inter. J. Molec. Sci*. **2014**, *15(2)*, 2024–2052.

2 Fredholm, B. B.; IJzerman, A. P.; Jacobson, K. A.; Linden, J.; Müller, C. E. International Union of Basic and Clinical Pharmacology. LXXXI. Nomenclature and classification of adenosine receptors—An Update. *Pharmacol. Rev.* **2011**, *63(1)*, 1.

[3] Gao, Z.-G.; Verzijl, D.; Zweemer, A.; Ye, K.; Göblyös, A.; IJzerman, A. P.; Jacobson, K. A. Functionally biased modulation of A3 adenosine receptor agonist efficacy and potency by imidazoquinolinamine allosteric enhancers. *Bioch. Pharmacol.* **2011**, *82(6)*, 658–668.

[4] Chen, J. F.; Eltzschig, H. K.; Fredholm, B.B. Adenosine receptors as drug targets – what are the challenges? *Nat. Rev. Drug Discov.* **2013**, *12(4)*, 265–86.

[5] St Hilaire, C.; Carroll, S. H.; Chen, H.; Ravid, K. C. Mechanisms of induction of adenosine receptor genes and its functional significance. *J. Cell Physiol.* **2009**, *218(1)*, 35–44.

[6] Baraldi, P.; Tabrizi, M.; Gessi, S.; Borea, P. Adenosine receptor antagonists: translating medicinal chemistry and pharmacology into clinical utility. *Chem. Rev.* **2008**, *108*, 238–263.

[7] Jacobson, K. A.; Müller, C. E. Medicinal chemistry of adenosine, P2Y and P2X receptors. *Neuropharmacology* **2016**, *104*, 31–49.

[8] Mizuno, Y.; Hasegawa, K.; Kondo, T.; Kuno, S.; Yamamoto, M. Clinical efficacy of istradefylline (KW-6002) in Parkinson's disease: a randomized, controlled study. *Mov. Disord.* **2010**, *25(10)*, 1437–1443.

[9] Sousa, J. B.; Diniz, C. The adenosinergic system as a therapeutic target in the vasculature: new ligands and challenges. *Molecules* **2017**, *22(5)*, 752–779.

[10] Vecchio, E. A.; Baltos, J. A.; Nguyen, A. T. N.; Christopoulos, A.; White, P. J.; May, L.T. New paradigms in adenosine receptor pharmacology: allostery, oligomerization and biased agonism. *Br. J. Pharmacol.* **2018**, *175(21)*, 4036–4046.

[11] Melani, A.; Pugliese, A. M.; Pedata, F. Adenosine receptors in cerebral ischemia. *Int. Rev. Neurobiol.* **2014**, *119*, 309–348.

12 Rivkees, S. A.; Thevananther, S.; Hao, H. Are A3 adenosine receptors expressed in the brain? *Neuroreport.* **2000**, *11(5)*, 1025–1030.

13 Borea, A. P.; Varani, K.; Vincenzi, F.; Baraldi, P. G.; Tabrizi, M. A.; Merighi, S.; Gessi, S. The A3 receptor: history and perspectives. *Pharmacol. Rev.* **2015**, *67(1)*, 74–102.

14 Fishman, P.; Cohen, S. The A3 adenosine receptor (A3AR): therapeutic target and predictive biological marker in rheumatoid arthritis. *Clin. Rheumatol.* **2016**, *35(9)*, 2359–2362.

15 Bagatini, M. D.; Dos Santos, A. A.; Cardoso, A. M.; Mânica, A.; Reschke, C. R.; Carvalho, F. B. The Impact of purinergic system enzymes on noncommunicable, neurological, and degenerative diseases. *J. Immunol. Res.* **2018**, 4892473.

16 Vazquez-Rodriguez, S.; Matos, M. J.; Santana, L.; Uriarte, E.; Borges, F.; Kachler, S.; Klotz, K.-N. Chalcone-based derivatives as new scaffolds for hA3 adenosine receptor antagonists. *J. Pharm. Pharmacol.* **2013**, *65*, 697–703.

17 Fonseca, A.; Matos, M. J.; Vilar, S.; Kachler, S.; Klotz, K.-N.; Uriarte, E.; Borges, F. Coumarins and adenosine receptors: New perceptions in structure-affinity relationships. *Chem. Biol. Drug Des.* **2018**, *91*, 245–256.

18 Matos, M. J.; Hogger, V.; Gaspar, A.; Kachler, S.; Borges, F.; Uriarte, E.; Santana, L.; Klotz, K.-N. Synthesis and adenosine receptors binding affinities of a series of 3-arylcoumarins. *J. Pharm. Pharmacol.* **2013**, *65*, 1590–1597.

19 Matos, M. J.; Gaspar, A.; Kachler, S.; Klotz, K.-N.; Borges, F.; Santana, L.; Uriarte, E. Targeting adenosine receptors with coumarins: synthesis and binding activities of amide and carbamate derivatives. *J. Pharm. Pharmacol.* **2013**, *65*, 30–34.

20 Matos, M. J.; Vilar, S.; Kachler, S.; Celeiro, M.; Vazquez-Rodriguez, S.; Santana, L.; Uriarte, E.; Hripcsak, G.; Borges, F.; Klotz, K.-N. Development of novel adenosine receptor ligands based on the 3-amidocoumarin scaffold. *Bioorg. Chem.* **2015**, *61*, 1–6.

[21] Matos, M. J.; Vilar, S.; Kachler, S.; Fonseca, A.; Santana, L.; Uriarte, E.; Borges, F.; Tatonetti, N. P.; Klotz, K.-N. Insight into the interactions between novel coumarin derivatives and human A3 adenosine receptors. *ChemMedChem* **2014**, *9*, 2245–2253.

[22] Matos, M. J.; Varela, C.; Vilar, S.; Hripcsak, G.; Borges, F.; Santana, L.; Uriarte, E.; Fais, A.; Di Petrillo, A.; Pintus, F.; Era, B. Design and discovery of tyrosinase inhibitors based on a coumarin scaffold. *RSC Adv.* **2015**, *5*, 94227–94235.

[23] Matos, M. J.; Santana, L.; Uriarte, E.; Delogu, G.; Corda, M.; Fadda, M. B.; Era, B.; Fais, A. New halogenated phenylcoumarins as tyrosinase inhibitors. *Bioorg. Med. Chem. Lett.* **2011**, *21(11)*, 3342–3345.

[24] Viña, D.; Matos, M. J.; Ferino, G.; Cadoni, E.; Laguna, R.; Borges, F.; Uriarte, E.; Santana, L. 8-Substituted 3-arylcoumarins as potent and selective MAO-B inhibitors: synthesis, pharmacological evaluation, and docking studies. *ChemMedChem* **2012**, *7(3)*, 464–470.

[25] Matos, M. J.; Perez-Cruz, F.; Vazquez-Rodriguez, S.; Uriarte, E.; Santana, L.; Borges, F.; Olea-Azar, C. Remarkable antioxidant properties of a series of hydroxy-3-arylcoumarins. *Bioorg. Med. Chem.* **2013**, *21(13)*, 3900–3906.

[26] Matos, M. J. CCDC 1937910: Experimental crystal structure determination. *CSD Commun.* **2019**, DOI: 10.5517/ccdc.csd.cc231k7z.

[27] Matos, M. J.; Santana, L.; Uriarte, E. 3-Phenylcoumarin. *Acta Cryst.* **2012**, *E68*, o2645.

[28] Klotz, K.-N.; Hessling, J.; Hegler, J.; Owman, C.; Kull, B.; Fredholm, B. B.; Lohse, M. J. Comparative pharmacology of human adenosine receptor subtypes - characterization of stably transfected receptors in CHO cells. *Naunyn Schmiedebergs Arch. Pharmacol.* **1997**, *357*, 1–9.

[29] Klotz, K.-N.; Falgner, N.; Kachler, S.; Lambertucci, C.; Vittori, S.; Volpini, R.; Cristalli, G. [3H]HEMADO–a novel tritiated agonist selective for the human adenosine A3 receptor. *Eur. J. Pharmacol.* **2007**, *556*, 14–18.

[30] Gazoni, L. M.; Walters, D. M.; Unger, E. B.; Linden, J.; Kron, I. L.; Laubach, V. E. Activation of A1, A2A, or A3 adenosine receptors attenuates lung ischemia-reperfusion injury. *J. Thorac. Cardiovasc. Surg.* **2010**, *140(2)*, 440–446.

[31] Buccioni, M.; Marucci, G.; Dal Ben, D.; Giacobbe, D.; Lambertucci, C.; Soverchia, L.; Thomas, A.; Volpini, R.; Cristalli, G. Innovative functional cAMP assay for studying G protein-coupled receptors: application to the pharmacological characterization of GPR17. *Purinerg. Signal.* **2011**, *7*, 463-468.

[32] Cagide, F.; Gaspar, A.; Reis, J.; Chavarria, D.; Vilar, S.; Hripcsak, G.; Uriarte, E.; Kachler, S.; Klotz, K.-N.; Borges, F.; Navigating in chromone chemical space: discovery of novel and distinct A3 adenosine receptor ligands. *RSC Adv.* **2015**, *5*, 78572–78585.

[33] Schrödinger suite 2014-3, Schrödinger, LLC, New York, USA, 2014. Available at: http://www.schrodinger.com/.

[34] Jaakola, V. P.; Griffith, M. T.; Hanson, M. A.; Cherezov, V.; Chien, E. Y.; Lane, J. R.; Ijzerman, A. P.; Stevens, R. C. The 2.6 angstrom crystal structure of a human A2A adenosine receptor bound to an antagonist. *Science* **2008**, *322*, 1211–1217.

[35] Congreve, M.; Andrews, S. P.; Doré, A. S.; Hollenstein, K.; Hurrell, E.; Langmead, C. J.; Mason, J. S.; Ng, I. W.; Tehan, B.; Zhukov, A.; Weir, M.; Marshall, F. H. Discovery of 1,2,4-triazine derivatives as adenosine A2A antagonists using structure based drug design. *J. Med. Chem.* **2012**, *55*, 1898–1903.

[36] Jaakola, V. P.; Lane, J. R.; Lin, J. Y.; Katritch, V.; Ijzerman, A. P.; Stevens, R. C. Ligand binding and subtype selectivity of the human A2A adenosine receptor:

identification and characterization of essential amino acid residues. *J. Biol. Chem.* **2010**, *285*, 13032–13044.

37 Gaspar, A.; Reis, J.; Kachler, S.; Paoletta, S.; Uriarte, E.; Klotz, K.-N.; Moro, S.; Borges, F. Discovery of novel A3 adenosine receptor ligands based on chromone scaffold. *Biochem. Pharmacol*. **2012**, *84(1)*, 21–29.

38 Alcaro, S.; Coleman, R. S. A molecular model for DNA cross-linking by the antitumor agent azinomycin B. *J. Med. Chem.* **2000**, *43(15)*, 2783–2788.

39 Perola, E.; Charifson, P. S. Conformational analysis of drug-like molecules bound to proteins: an extensive study of ligand reorganization upon binding. *J. Med. Chem.* **2004**, *47(10)*, 2499–2510.

40 Schiebel, J.; Gaspari, R.; Wulsdorf, T.; Ngo, K.; Sohn, C.; Schrader, T. E.; Cavalli, A.; Ostermann, A.; Heine, A.; Klebe, G. Intriguing role of water in protein-ligand binding studied by neutron crystallography on trypsin complexes. *Nat. Commun.* **2018**, *9(1)*, 3559.

41 Walki, S.; Naveen, S.; Kenchanna, S.; Mahadevan, K. M.; Kumara, M. N.; Lokanath, N. K. Crystal structure of 8-ethoxy-3-(4-nitrophenyl)-2*H*-chromen-2-one. *Acta Crystallogr. E Crystallogr. Commun.* **2015**, *71(11)*, o860–o861.

42 Valenti, P.; Rampa, A.; Budriesi, R.; Bisi A.; Chiarini, A. Coumarin 1,4-dihydropyridine derivatives. *Bioorg. Med. Chem.* **1998**, *6*, 803–810.

43 Nemeryuk, M. P.; Dimitrova, V. D.; Sedov, A. L.; Anisimova, O. S.; Traven, V. F. New approach to the synthesis of 3-arylcoumarins. Reaction of 3-acyl and 3-ethoxycarbonyl-coumarins with hydrazide of *p*-nitrophenylacetic acid. *Chem. Heteroc. Comp.* **2002**, *38(2)*, 249–250.

44 Jafarpour, F.; Zarei, S.; Olia, M. B. A.; Jalalimanesh, N.; Rahiminejadan, S. Palladium-catalyzed decarboxylative cross-coupling reactions: a route for regioselective functionalization of coumarins. *J. Org. Chem.* **2013**, *78*, 2957−2964.

45 Bulut, M.; Erk, C. The synthesis of novel crown ethers, part IX, 3-phenyl chromenone-crown ethers *J. Heteroc. Chem.* **2001**, *38(6)*, 1291–1295.

46 Gunduz, C.; Bulut, M. Synthesis of 7,8-dihydroxy-3-(3,4-dihydroxyphenyl)-2*H*-chromen-2-one derivatives of crown ethers. *J. Heteroc. Chem.* **2009**, *46(1)*, 105–107.

47 Katritch, V.; Kufareva, I.; Abagyan, R. Structure based prediction of subtype-selectivity for adenosine receptor antagonists. *Neuropharmacology* **2011**, *60*, 108–115.

48 MOE, version 2011.10; Chemical Computing Group, Inc.: Available at: http://www.chemcomp.com.

49 Waterhouse, A.; Bertoni, M.; Bienert, S.; Studer, G.; Tauriello, G.; Gumienny, R.; Heer, F. T.; de Beer, T. A. P.; Rempfer, C.; Bordoli, L.; Lepore, R.; Schwede, T. SWISS-MODEL: homology modelling of protein structures and complexes. *Nucleic Acids Res.* **2018**, *46(W1)*, W296–W303.

50 Glukhova, A.; Thal, D. M.; Nguyen, A. T.; Vecchio, E. A.; Jörg, M.; Scammells, P. J.; May, L. T.; Sexton, P. M.; Christopoulos, A. Structure of the Adenosine A1 Receptor Reveals the Basis for Subtype Selectivity. *Cell* **2017**, *168(5)*, 867–877.

Table of Contents graphic